

NINTH EUROPEAN ROTORCRAFT FORUM

Paper No. 27

VISUAL AIDS FOR FUTURE HELICOPTERS

H.-D.V. Böhm

R.-D. v. Reth

Messerschmitt-Bölkow-Blohm GmbH

MUNICH, GERMANY

September 13 - 15, 1983

STREZA, ITALY

ASSOCIAZIONE INDUSTRIE AEROSPAZIALI

ASSOCIAZIONE ITALIANA DI AERONAUTICA ET ASTRONAUTICA

VISUAL AIDS FOR FUTURE HELICOPTERS

H.-D.V. Böhm

R.-D. v. Reth

Messerschmitt-Bölkow-Blohm GmbH

Munich, Germany

Abstract

In the past years MBB has carried out numerous flight trials involving different night vision systems for various applications and missions. The experiments not only covered different night vision sensors for pilot or observer, but also the aspects of different displays and stabilized and steerable platforms.

Recently a Pilot Visionics System (PVS) was tested on a MBB-Bo 105 helicopter. This PVS included a Helmet-Mounted Sight/Display (HMS/D), a stabilized steerable platform with a wide field of view FLIR and LLLTV camera. For comparison purposes, a Head-down Display (HDD) was also used. The FLIR and LLLTV images could be displayed alternately to allow for direct comparison during the flight tests. In various tests, a direct comparison between Night Vision Goggles (NVG), FLIR and LLLTV camera was carried out.

In more recent tests a newly designed FLIR camera with a steerable platform called "Piloten Infrarot Sicht-Anlage" (PISA) using an especially large field of view ($30^\circ \times 60^\circ$) was also investigated.

The major results of the PVS and PISA trials are presented and discussed in this paper. As one result, it was found that the FLIR generally gave a better image when directly compared with the LLLTV camera. It was also confirmed that NVG are quite effective, even when compared to relatively complex systems using a steerable platform with FLIR sensor, an HMS/D and separate display equipment.

In addition to these experiments, a number of system configurations and combinations for future helicopters are evaluated. It will be seen that the NVG are a strong contender for a large number of applications and offer a cost-effective solution for the piloting task. As far as the observation task is concerned, the feasibility of a complex sensor package on the rotormast has already been demonstrated (ref. 2, 5 and 6).

1. Introduction

Since 1981, MBB has tested three different night vision systems on the Bo 105 flying laboratory in order to evaluate specifications and to gain experience of such equipment for future developments. The aim of the flight trials was to investigate the extension of the helicopter's mission spectrum to flying at night and in adverse weather conditions.

An observation system, OPHELIA, was configured as a mast-mounted observation platform (ref. 2, 5, 6 and 11) and two pilot vision systems were mounted in the helicopter nose (ref. 5, 9, 10 and 11). The two pilot vision systems, as visual aids for future helicopters, will be described in more detail in this paper. Trials were performed during the period July/August 1982 on a Pilot Visionics System (PVS), sponsored by the German Ministry of Research and Technology (BMFT), and during the period April/May 1983 on a "Piloten Infrarot Sicht-Anlage" (PISA). In both instances, a Bo 105 was used as flying test bed.

The PVS comprises a Helmet-Mounted Sight and Display (HMS/D) with electro-magnetic head position measurement, a stabilized steerable platform with two electro-optical sensors, a FLIR (26° x 38°) and an LLLTV camera (30° x 40°). The sensor line of sight (LOS) on the platform follows exactly the pilot's head movements by means of the measurement system. Images of the outside world are relayed to the pilot from the sensors and are displayed on a miniature cathode ray tube (CRT) fitted to his helmet (HMD). For comparison purposes, a Head-down Display (HDD) was installed in front of the pilot. The sensor images on the displays could be superimposed with two different computer generated symbologies: Cruise and Transition/Hover. Additional tests were conducted to compare Night Vision Goggles (NVG) with the electro-optical sensors of the PVS. 46 flight tests were performed, including 14 night flights. The FLIR and the LLLTV images could be displayed alternately to allow for direct comparison during the flight tests. The images were additionally recorded on video-tape. For post-flight evaluation a magnetic tape recorder was fitted to register 12 signals from the helmet, the controller and the platform, together with helicopter motion and the external illumination levels.

A simpler pilot vision system is demonstrated by PISA. A beeper and a reset switch mounted on the collective stick were used for platform steering. The platform contained a wide angle FLIR (30° x 60°) whose image was displayed on a large-screen HDD installed in front of the pilot. A new Cruise symbology could be superimposed on the image. 18 flight tests including 4 night flights were conducted with PISA.

2. Description of the Pilot Visionics System (PVS)

2.1 FLIR and LLLTV system with coupled HMS/D

In addition to MBB, five companies from Germany, France and Great Britain participated in the project. The companies involved were Ferranti for the HMS/D; SFIM for the stabilized platform; Leitz who are licenced to produce the Barr & Stroud IR 18 Mark II infrared camera; AEG-Telefunken for the LLLTV camera and VDO for the HDD and the symbol generator (SG).

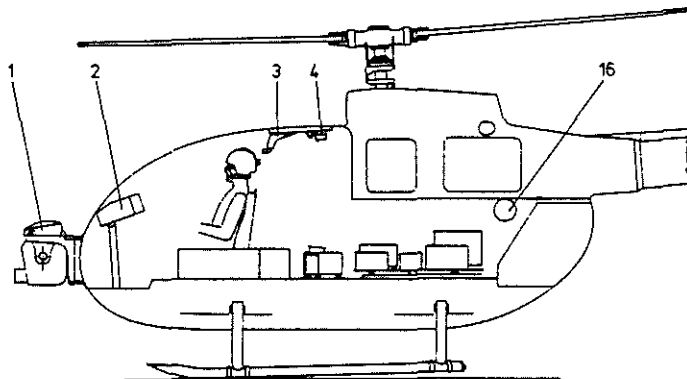
Fig. 1 shows the helicopter with the nose-mounted platform (PVS) and Fig. 2 a drawing of the helicopter with the PVS components fitted (see ref. 7 and 8).



Fig. 1: Bo 105 with the nose-mounted platform (PVS)

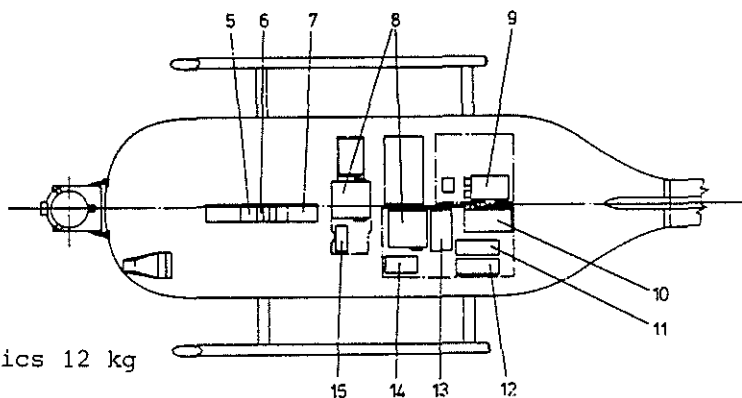
Fig. 2: PVS on the Bo 105

- 1 - steerable stabilized platform with FLIR and LLLTV camera
- 2 - HDD
- 3 - electro-magnetic radiator
- 4 - interface helmet/fuselage
- 5, 6, 7 - PVS control units
- 8 - two video recorders
- 9 - converter
- 10 - symbol generator
- 11, 12 - HMS/D electronics
- 13 - platform electronics
- 14 - platform controller
- 15 - HDD interface
- 16 - 6 litre nitrogen bottle



The parameters of the platform are:

- o type PGS 402
- o two-axis gyro stabilization, accuracy: ± 1 mrad
- o diameter: 400 mm with room for the two optical sensors
- o displacement angles: AZ $\pm 90^\circ$, EL $+ 15^\circ / - 50^\circ$
- o slew rate: approx. $100^\circ/\text{sec}$
- o angular acceleration: $500^\circ/\text{sec}^2$
- o mass: platform 20 kg and electronics 12 kg



A block diagram of the HMS/D in conjunction with the platform is shown in Fig. 3.

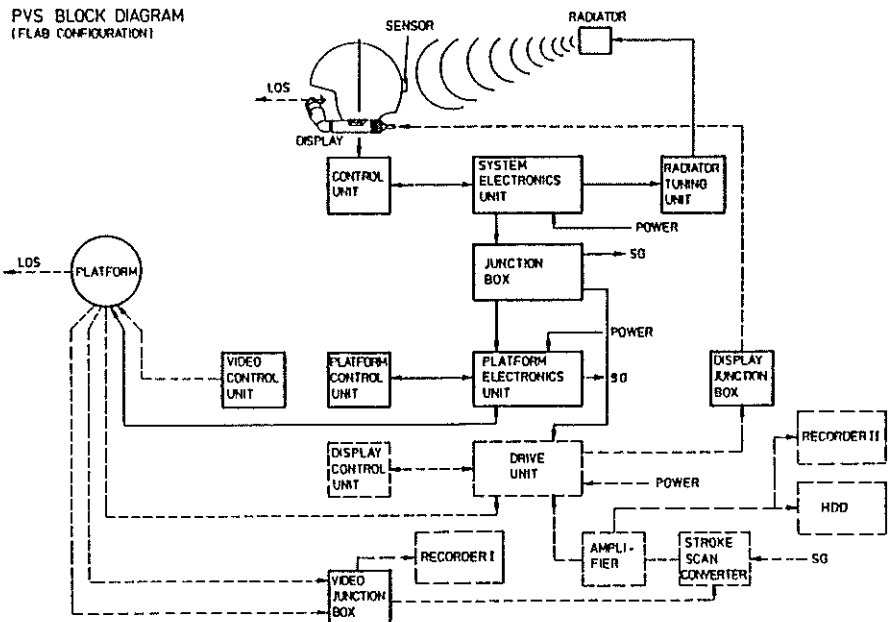


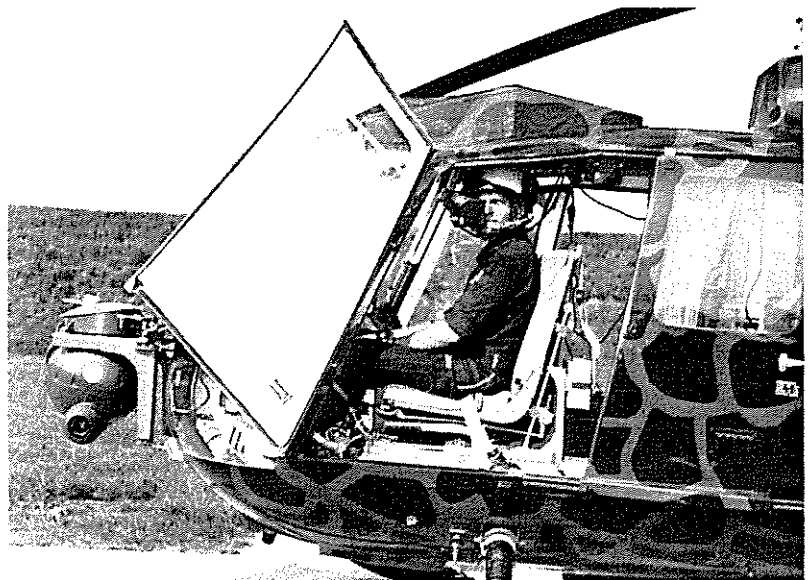
Fig. 3:

Block diagram of the HMS/D with the platform as used in the PVS

The HMS/D fulfils a dual function, firstly by determining the head motion of the crew member and secondly by displaying a sensor image directly in front of one eye. The HMS uses a three-axis electro-magnetic radiator attached to the helicopter cabin roof and a three-axis electro-magnetic sensor mounted on the pilot's helmet. The radiator emits a magnetic field which induces voltages in the sensor. The sensor signals are then processed by the electronics unit to determine the position and attitude of the sensor relative to the radiator. Fig. 4 shows the HMS/D in conjunction with the steerable platform. Between the HMS and the platform lies a controller which relays the HMS signals to the platform. The optical sensor LOS follows exactly the pilot head movements. The HMS/D itself is seen in Fig. 5 (see ref. 3).

Fig. 4:

Pilot with an HMS/D (Ferranti) in conjunction with a visually-coupled platform (SFIM)



A cockpit mapping procedure is initially required to set up the HMS and the installation of the radiator also requires some special precautions with respect to magnetic material in the areas immediately adjacent to it. The arrangement for the cockpit mapping procedure, with the sensor on a moveable carriage and the radiator supported from the roof on a composite material structure, is shown in Fig. 6.

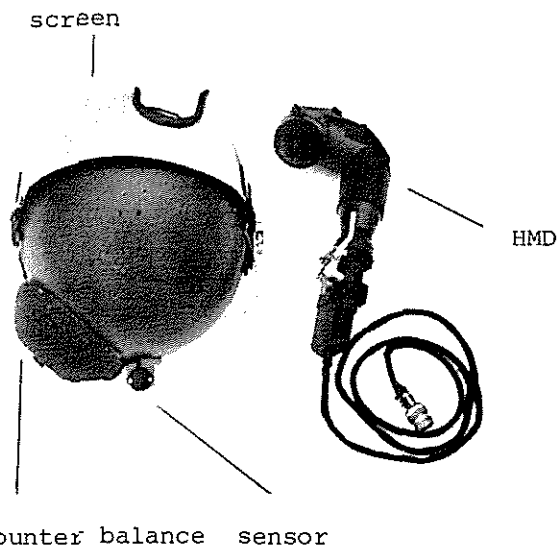


Fig. 5: Helmet with HMS/D (Ferranti)

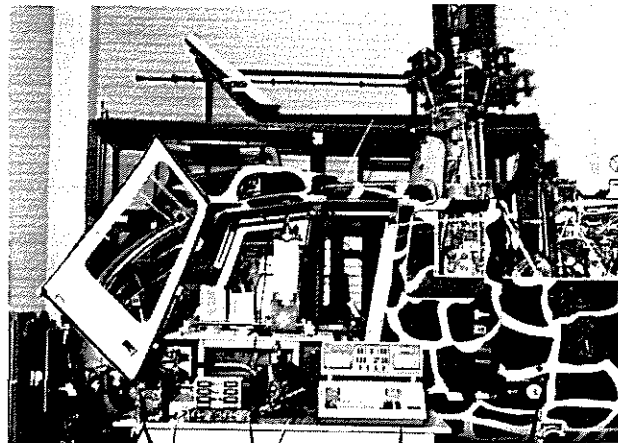


Fig. 6: Cockpit mapping for the electro-magnetic HMS/D (Ferranti)

The parameters of the HMS/D are:

- HMS

- o electro-magnetic principle for head position determination
- o angular coverage: $\pm 180^\circ$ in AZ and $\pm 90^\circ$ in EL
- o max. slew rate: $100^\circ/\text{sec}$
- o accuracy: 0.5° CEP
- o mass: 15.7 kg incl. electronics

- HMD

- o miniature CRT 19 mm diameter
- o FOV: $30^\circ \times 40^\circ$ (vert. x horizont.)
- o magnification: x 1
- o max. eye relief: 104 mm
- o display colour: phosphor green
- o mass: 13.8 kg incl. electronics

The system is bore-sighted before take-off by means of a single-point source. Re-alignment of the system can be carried out during flight if necessary. This prototype, monocular display - HMD - is fitted to the modified pilot's helmet and is viewed with the right eye. The display is focused at infinity. The image is roll-stabilized to keep the sensor image horizon aligned with the natural horizon when the pilot moves his head in roll.

Two electro-optical sensors are installed in the platform. Modification of the platform cowling, see Figs. 4 and 7, allows the simultaneous installation of the FLIR, IR 18 Mk II, and the LLLTV camera, PA. These two cameras operate on two different physical principles. The FLIR detects the Planck radiation in the 8 - 13 μm spectral region while the LLLTV camera amplifies the existing light (reflection) similar to the NVG in the 0.5 - 0.9 μm region.

The parameters of the FLIR are:

- o type IR 18 Mark II
- o spectral region: 8 - 13 μm
- o FOV: $26^\circ \times 38^\circ$, EP 14.5 mm
- o IFOV: 1.44 mrad
- o magnification: x 1
- o 4 TED (Sprite)-detectors (62.5 x 700 μm), cooled by nitrogen supplied from a 6 litre bottle
- o quasi serial/parallel scanning
- o polygon, n = 6, 651 Hz
- o 5 contrast steps, variable brightness control
- o CCIR standard
- o mass: 6.8 kg incl. electronics

The parameters of the LLLTV are:

- o type PA
- o spectral region: 0.5 - 0.9 μm
- o FOV: $30^\circ \times 40^\circ$
- o magnification: x 1
- o Ebsicon-tube with an image intensifier
- o CCIR standard
- o limiting ambient light level: approx. 3 mlux
- o mass: 8.3 kg incl. electronics

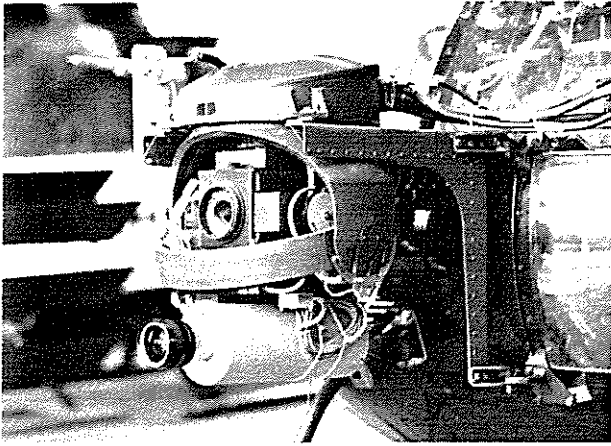


Fig. 7:

PVS platform with cowling removed. FLIR (Leitz/Barr & Stroud) above and LLLTV (AEG-Telefunken) below. The platform mounting is also visible.

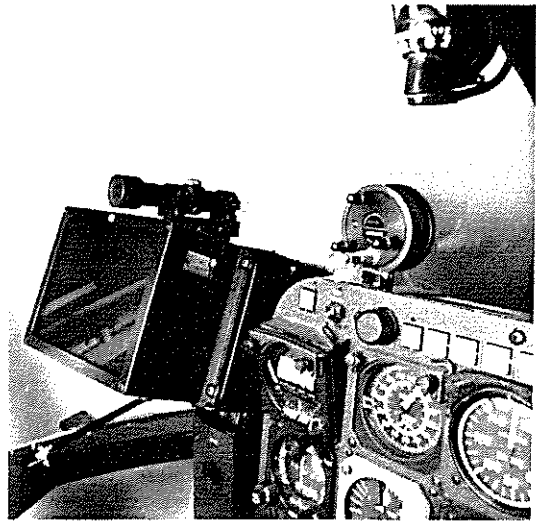


Fig. 8:

HDD (VDO) for comparison purposes, single-point boresighting module, illumination meter and parts of the instrument panel

Fig. 8 shows the 8"-HDD (phosphor green screen) used for comparison with the HMD, together with the single-point boresighting module.

2.2 Night vision goggles (NVG)

When investigating visual aids for piloting, NVG with light intensifying tubes have of course also to be considered, their major advantages being a relatively large FOV, a direct coupling with the head motion, their simplicity and consequently comparatively low cost. Two different helmet-mounted NVG, each with tubes of 2nd and 3rd generations, were used: an Elektro-Spezial NVG of the type BM 8028 with 48° FOV and a Bell & Howell NVG of the type ANVIS (on loan from RAE, Farnborough) with 40° FOV, see Figs. 9 and 10. The GaAs photocathodes of the 3rd generation tubes have more sensitivity around the 0.8 and 0.9 μm wavelength than the S 25 photocathodes of the 2nd generation tubes. The 3rd generation tubes can be used down to an illumination level of 0.5 mlux.



Fig. 9:

Helmet-mounted NVG of the type BM 8028 (Elektro-Spezial). 2nd and 3rd gen. tubes were used.

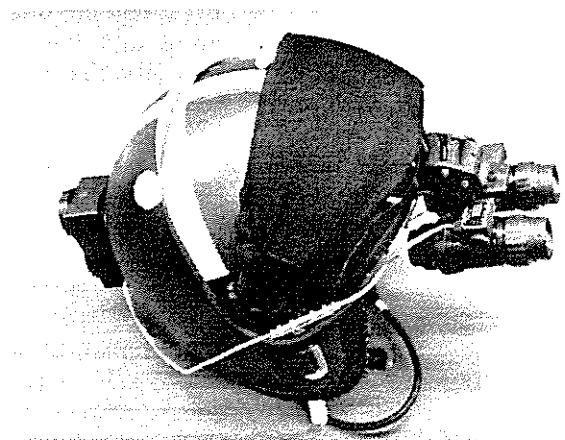


Fig. 10:

Helmet-mounted NVG of the type ANVIS (Bell & Howell). 2nd and 3rd gen. tubes were used.

3. Results of the PVS flight trials

3.1 FLIR and LLLTV system with coupled HMS/D

During the HMS cockpit mapping, the accuracy of this electro-magnetic device was determined. Fig. 11 shows one measurement cycle over the head-motion box of the helmet-mounted sensor. In this position, the sensor was only subjected to rotational movements.

The results are CEP = 0.28° with 126 measurement points for variable angles (AZ, EL) and CEP = 0.63° with 46 measurement points for sensor displacement of X, Y, Z (315, 380 and 130 mm) in the head-motion box. The first circular error probability (CEP) of 0.28° is the HMS error and the amount of the second error depends on the quality of the cockpit mapping. In this case, there was not enough time available for a second fit of cockpit mapping.

A metal hammer held in the proximity of the helmet did not greatly influence the magnetic field. The optical sensor LOS on the platform was found to change by approx. 1° . From Fig. 11, it can be seen that a permanent parallax existed between the LOS of the left eye and the optical sensor LOS on the platform. For example, if the pilot turns his helmet to AZ = 90° , this parallax error is 0.9° for an object at 100m distance. The flight trials showed however, that during manoeuvring, the pilot normally does not turn his head more than $\pm 60^\circ$ in AZ. Under $+15^\circ$ the parallax is zero. The boresighting error, (see Fig. 8) between the HMS/D with the sensor image and the left eye was CEP = 0.27° , evaluated from tests with 6 different people.

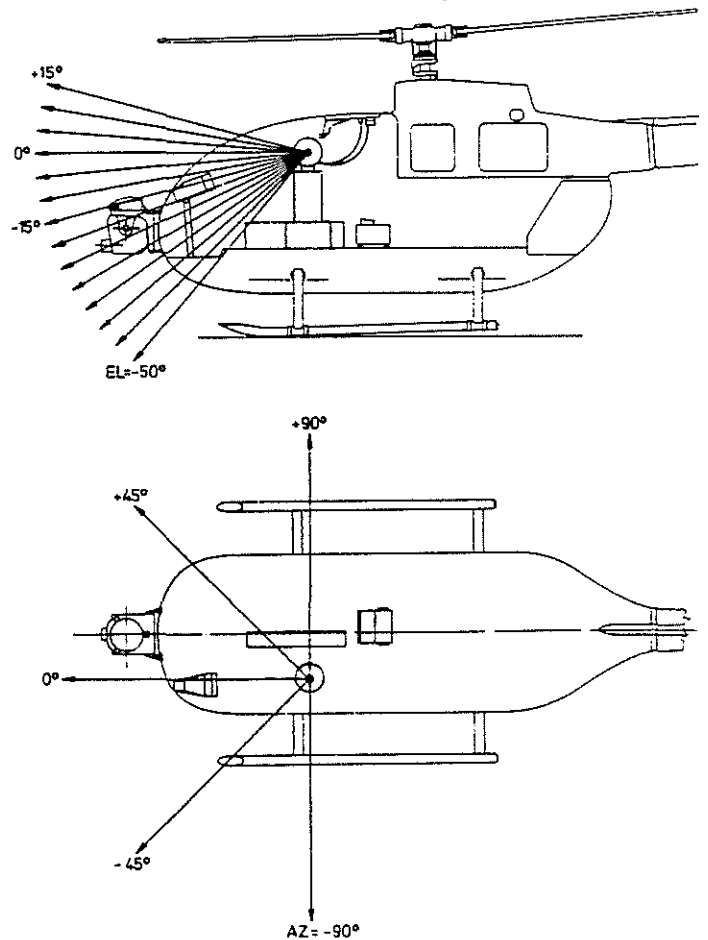


Fig. 11:

126 measurements of the HMS accuracy in the head-motion box for variable AZ and EL angles with fixed X, Y and Z.

The dynamic error between the HMS-LOS and the sensor LOS on the platform was established from the flight test results. 12 different signals were recorded on magnetic type during the trials. Fig. 12 picks out the HELM-AZ and HELM-EL movements during 200 seconds of manoeuvring flight at night. Not shown are the graphs for PLAT-AZ and PLAT-EL which are very similar. Over the 200 sec calculation time of this flight, the average LOS position for pilot 1 is HELM-AZ = $+0.7^\circ$ (max. 71.6° and min. -60.1°) and HELM-EL = -8.4° (max. 18.9° and min. -20.7°). It can be seen that for this flight segment, pilot 1 had an overall tendency to look downwards with an LOS at -8.4° . The altitude reading over this period was approx. 300 ft GND. Fig. 13 shows the distribution of HELM-AZ and HELM-EL motion for the same 200 seconds of flight. The larger open squares indicate the longest duration of stay in the particular angular field and the round black points the shortest duration of less than 0.6 sec in the total 200 sec.

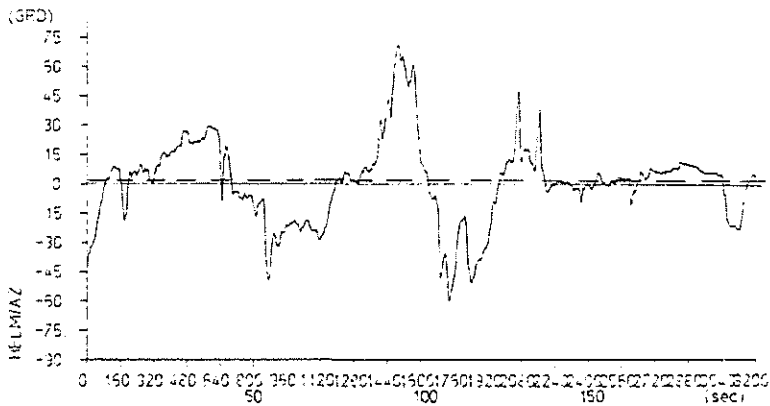


Fig. 12:

A 200 sec plot of HELM-AZ and HELM-EL movements for manoeuvring flight at night (pilot 1)

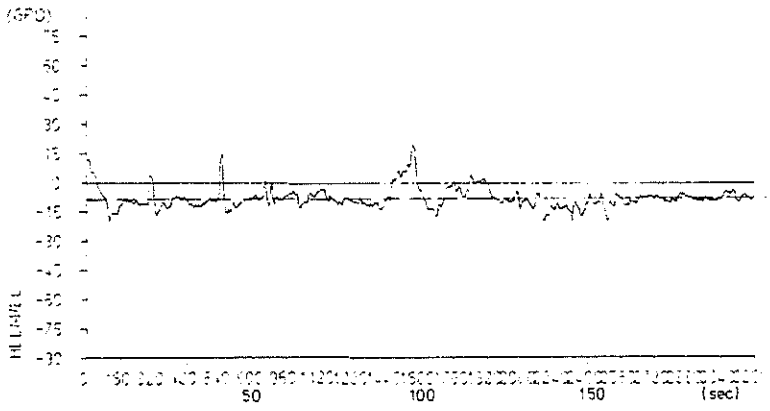


Fig. 14 uses the same form of representation as Fig. 13, this time for level flight. During this 200 second segment, pilot 1 tends to maintain his LOS more in the direction of flight in AZ, as he is not having to look out for obstacles. The average LOS positions for these 200 seconds are HELM-AZ = - 4.4° (max. 24.5° and min. - 41.8°) and HELM-EL = - 11.9° (max. - 3.7° and min. - 34.8°). The altitude was approx. 250 ft GND.

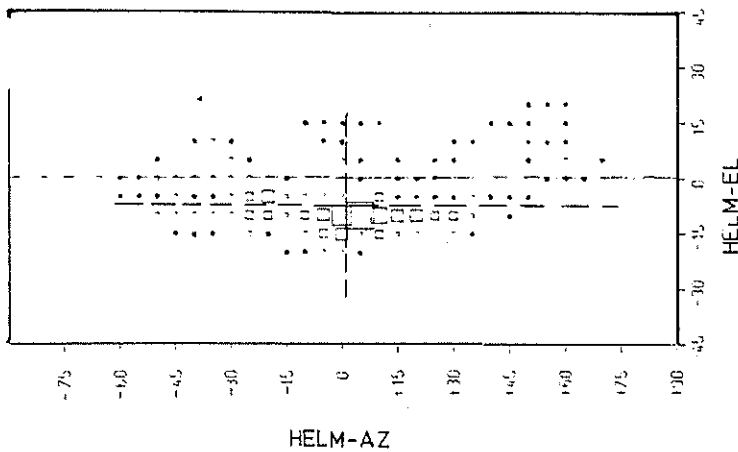


Fig. 13:

HELM-AZ and HELM-EL during manoeuvring night flight with pilot 1 (3200 computed points over 200 sec)

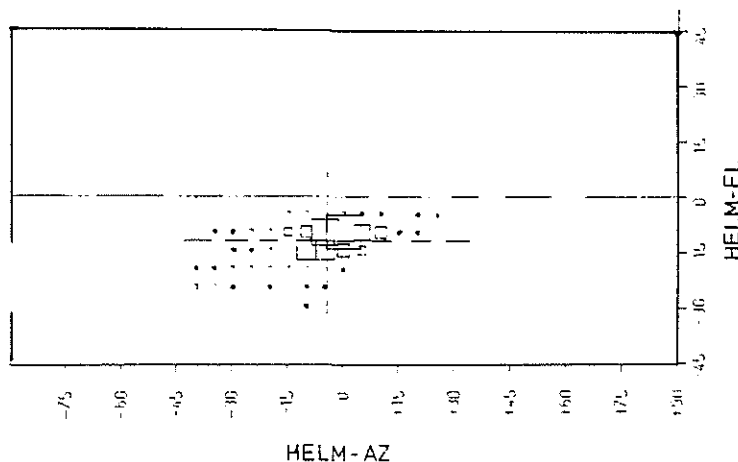


Fig. 14:

HELM-AZ and HELM-EL during level flight at night with pilot 1 (3200 computed points over 200 sec)

Fig. 15:

Comparison of HELM-AZ and PLAT-AZ for manoeuvring night flight with pilot 1. (3200 computed points over 200 sec). 82.3 % of the points lie on the straight line

Fig. 15 compares HMS movements in AZ to platform response, with the controller in the loop, for the manoeuvre night flight previously discussed. Of the 3200 calculated points over the 200 second period, 2635 lie on the straight line i.e. 82.3 %, with accuracy calculation at 16 Hz sampling rate. For level flight at night, 89.4 % of points lie on the straight line. Two other pilots were used to fly the same route. The calculated results of 6 night flights are shown in Table 1.

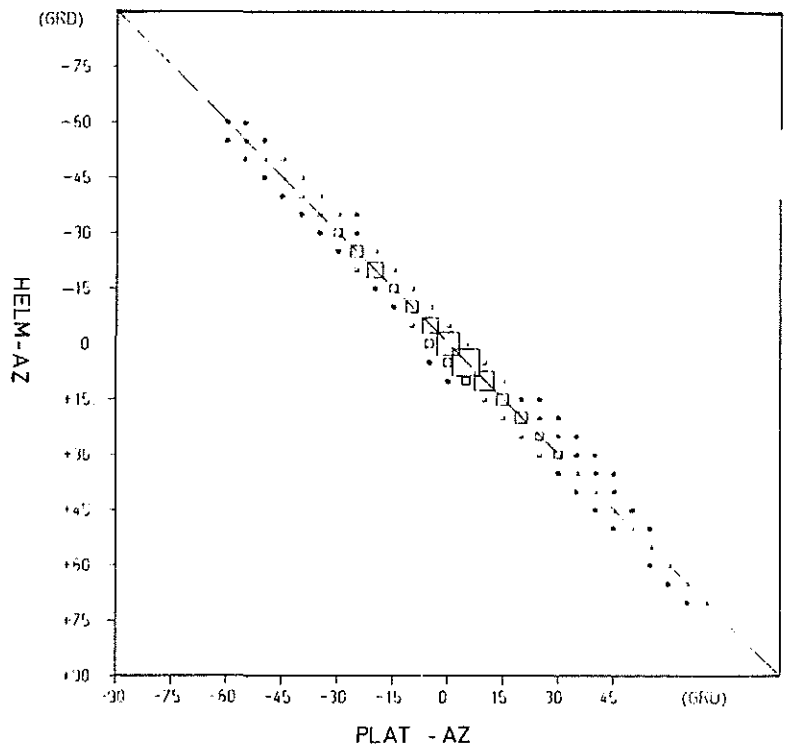


Table 1: HMS and platform average angular positions for 6 night flights including 2 manoeuvring flights; * standard deviation

	HELM-AZ	HELM-EL	PLAT-AZ	PLAT-EL	total time
max. average	+ 53.2°	+ 3.1°	+ 48.4°	+ 5.3°	1200 sec.
min. average	- 46.4°	- 37.5°	- 46.1°	- 31.8°	1200 sec.
average and s*	+ 3.9° ± 5.9°	- 13.4° ± 3.5°	+ 1.3° ± 5.1°	- 10.9° ± 2.6°	1200 sec.

Table 2: Measured HMS and platform speeds and accelerations

	HELM-AZ	HELM-EL	PLAT-AZ	PLAT-EL	total time
max. speed (°/s)	80.8	94.1	96.7	47.4	200 sec.
min. speed (°/s)	- 113.6	- 122.9	- 88.4	- 62.0	200 sec.
max. accel. (°/s ²)	1188	1321	490	505	200 sec.
min. accel. (°/s ²)	- 1188	- 1797	- 735	- 541	200 sec.

The dynamic accuracy of the HMS, the controller and the platform calculated with a sampling rate of 16 Hz, was approx. 2.5°. The average pilot LOS is approx. 13.4° downwards (at approx. 300 ft GND).

The measured speeds and accelerations of the HMS and the platform are listed in Table 2. The maximum and minimum values are calculated for a manoeuvring night flight of 200 seconds duration. They do not represent maximum and minimum values of the speed and acceleration. It can be seen from the Table 2 that the platform is slower in response than the HMS. The pilots were however satisfied with the platform dynamic response.

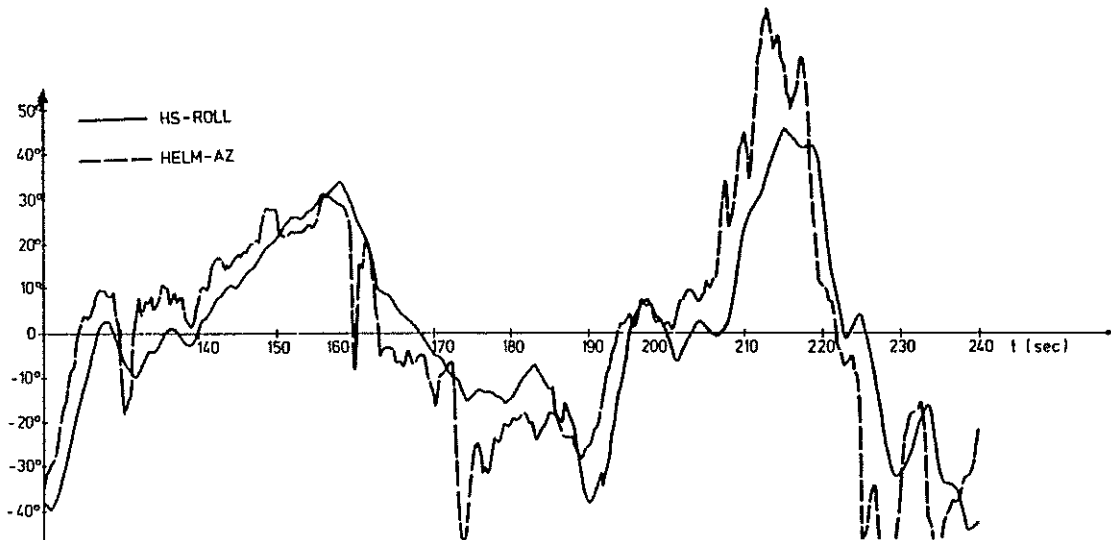


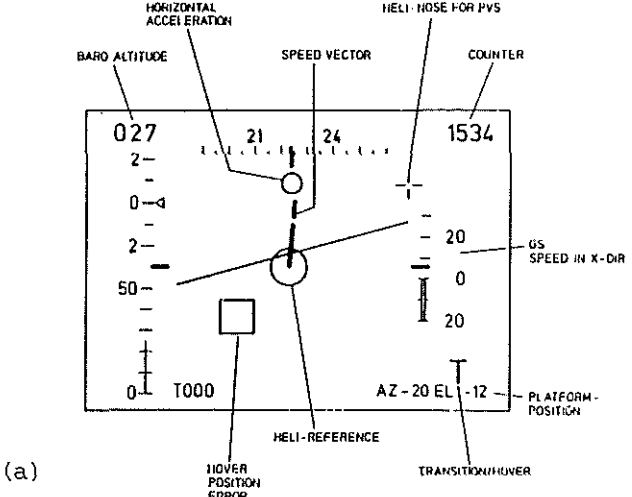
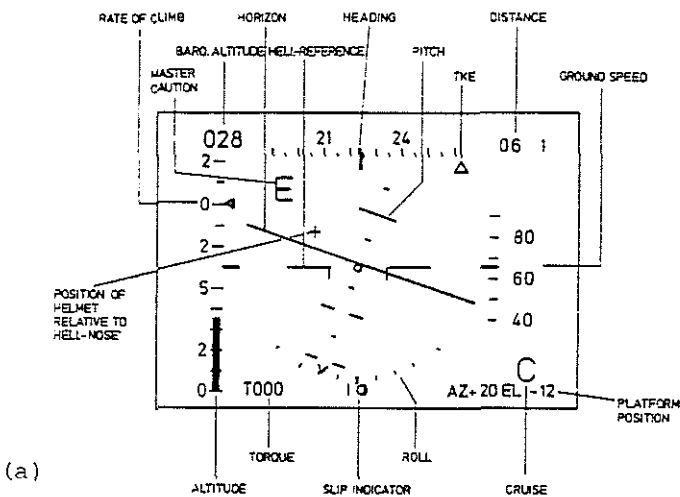
Fig. 16: HELM-AZ and the HELICOPTER-ROLL as functions of the time during a manoeuvre flight at night

Fig. 16 shows HELM-AZ and HELICOPTER-ROLL as functions of time during a 120 sec long manoeuvre flight at night. It can be seen that the pilot anticipates the HELICOPTER-ROLL manoeuvres by approx. 3 sec with head movements in AZ.

The maximum vibration level for the platform with payload was found to be 2.6 g in the Y-axis during flare. It was found that stabilization is not necessary for a platform with wide FOV sensors (i.e. 30° x 40°) but steering in AZ and in EL is required.

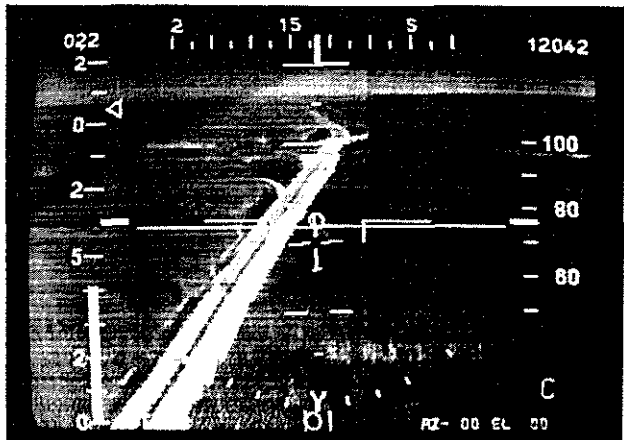
Both HMD resolution and FOV (30° x 40°) were deemed very good. HMS/D roll compensation was found to be absolutely essential to prevent disorientation. If the pilot e.g. at twilight, sees the natural horizon with his left eye and the artificial horizon in the sensor image with his right eye, he needs the roll compensation to keep both aligned. During twilight flights, the pilots experienced no rivalry between the left eye and the right eye with its displayed image. Inter-ocular rivalry is not expected either during the day or at night, as in the former case the left eye with view of the outside world is predominant, while during the latter the sensor image in the HMD is dominant. The Ferranti HMD used was a prototype unit - a weight reduction is essential for future developments.

The flight symbology was also assessed during the flight trials. The FLIR and LLLTV images could be superimposed with the selected symbology. The pilot was able to choose between either Cruise and Transition/Hover modes or no symbology (see Figs. 17 and 18). Different sizes of writing field could also be selected.

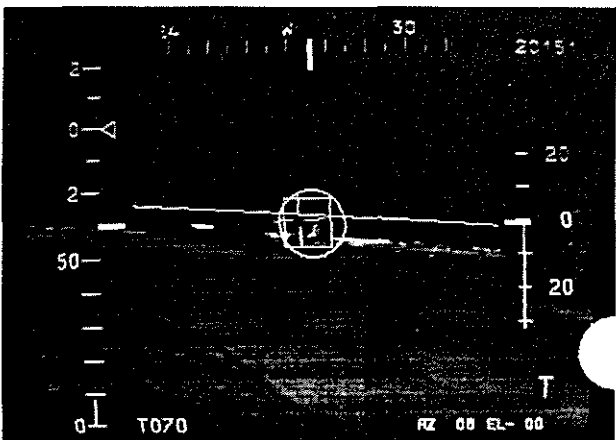


(a)

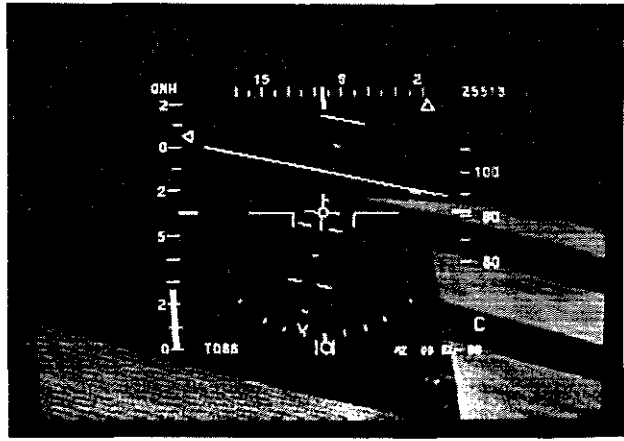
(a)



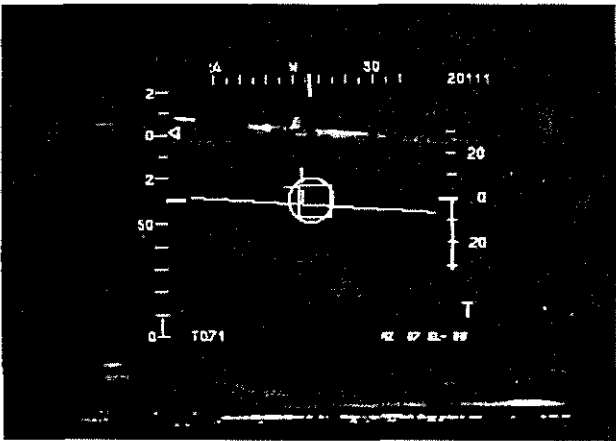
(b)



(b)



(c)



(c)

Fig. 17:

Cruise symbology, (c) shows the smaller writing fields

Fig. 18:

Transition/Hover symbology (c) shows the smaller writing field

Figs. 17 and 18 are self-explanatory with regard to symbols. Most pilots prefer to use the larger size of writing. They were satisfied with the Cruise mode but proposed changes to the Transition/Hover mode. It was not possible to hover in the latter mode without AFCS fitted on the Bo 105. The pilots also mentioned that they initially used the sensor image with the superimposed symbology as an IFR aid and

not to provide VFR information. As they gained more experience, they were able to fly the helicopter by means of the sensor image. The horizon is however sometimes very hard to identify in the image. Problems exist with the symbology brightness if the sensor image background is light.

Figs. 19 and 20 show two examples of the LLLTV and FLIR images. The pictures were photographed in the laboratory from a monitor replaying the video tapes. An exposure time of 1/30 sec was used. Black or white diagonal stripes can be seen in some of the images. These are a result of poor synchronisation between the TV picture (CCIR standard) and the camera shutter. The examples directly compare the LLLTV (left) and FLIR (right) images, recorded at night under identical environmental conditions. Not more than one second has elapsed between the images in both examples. Fig. 19 shows a motorway bridge on the Munich-Salzburg motorway. In the LLLTV image, the car headlights are seen to produce a blooming effect while in the FLIR image the cars appear as small white points on the motorway. In addition, the river, buildings, bridge and minor roads can very clearly be recognised. A landscape without man-made features is shown in Fig. 20. The trees and meadows appear life-like in the LLLTV image, while the FLIR image has a "photo negative" quality. The "warm" river (white) is clearly seen in the centre of the thermal image. It was generally found during the flight trials, that the geometric resolution and contrasts of the FLIR were better than those of the LLLTV camera. Under 10 mLux, the LLLTV shows snow-like effects in the image while in most cases the blooming effects are disturbing. The FLIR displayed a slight Narcissus effect resulting from a wrongly tilted Ge-window in the platform cowling. Both sensors had problems with the brightness control in the case were they were steered quickly from the sky to the ground. The other features of the camera were judged to be satisfactory .

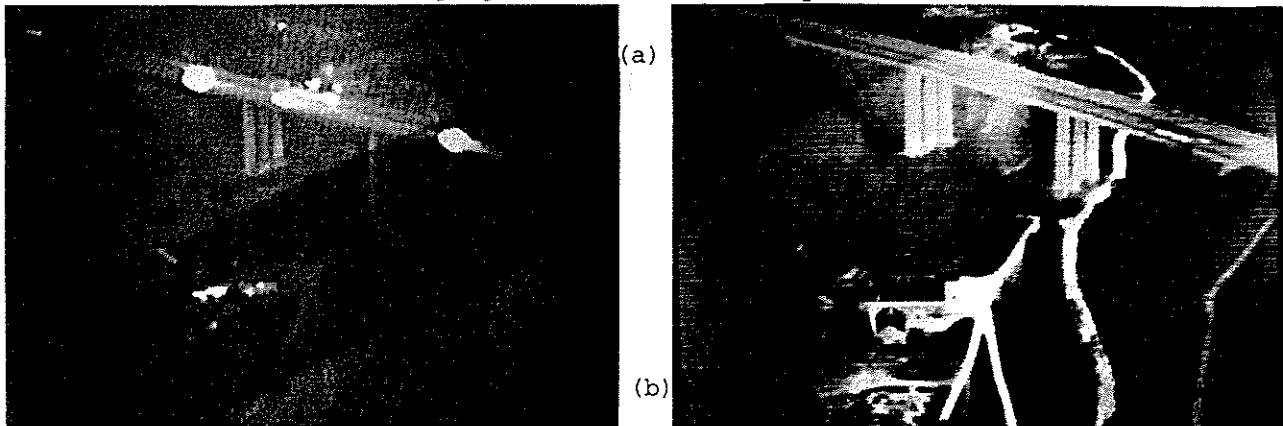


Fig. 19: Direct comparison of LLLTV (a) and FLIR (IR 18 Mk II), (b) images during the same PVS night flight (approx. 200 mLux). Images show a motorway bridge.

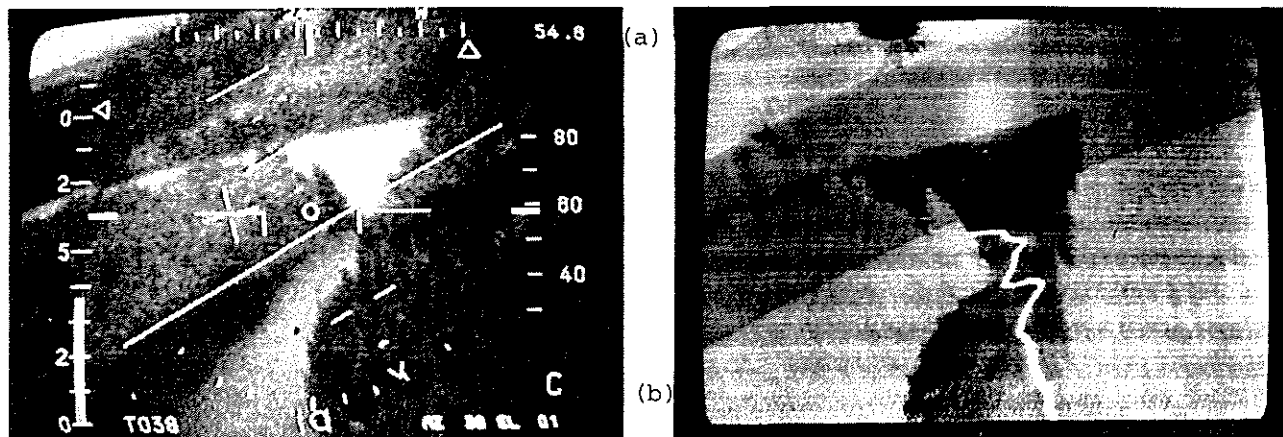


Fig. 20: Direct comparison of LLLTV (a) and FLIR (IR 18 Mk II), (b) images during the same PVS night flight (approx. 500 mLux). Images show a valley with surrounding woods.

3.2 Night vision goggles

Figs. 21 and 22 show views through two different NVG. The objects were photographed through one tube of each NVG. For these tests both NVG were fitted with tubes of the third generation. The picture taken with the Elektro-Spezial goggle shows the Bo 105-S1 helicopter on the landing pad. A weak blooming effect is present from the tower lights. The constellation Orion was taken through the Bell & Howell NVG. It was possible to detect many more of the less bright stars with the goggles than with the naked eye. Of interest here are the reddish Betelgeuze and bluish Rigel stars. Rigel ($T = 12000 \text{ K}$) appears brighter than Betelgeuze ($T = 3300 \text{ K}$) in the visible spectrum, but through the NVG the reverse is true. This is understandable if the sensitivity of the 3rd generation tubes is compared with the Planck radiation curve maxima of both stars of $\lambda_{\text{max}} = 0.24 \mu\text{m}$ for Rigel and $0.88 \mu\text{m}$ for Betelgeuze (comp. Fig. 23).



Fig. 21:

View through the Elektro-Spezial BM 8028 NVG with 3rd gen. tubes. The helicopter and a tower with lights can be seen. Blooming effects are insignificant because of multichannel plate saturation



Fig. 22:

View through the Bell & Howell ANVIS NVG with 3rd gen. tubes. The constellation of Orion can be seen with the reddish Betelgeuze (upper left) and the bluish Rigel (lower right) stars

Fig. 23 additionally contains the day and night sensitivity of the eyes, a cut-off filter curve and the night sky irradiance. The cut-off filter is shown in Fig. 24 in front of the NVG, used for producing compatibility with cockpit night illumination (ref. 1 and 4). It is not necessary to make frequent focal adjustments with this helmet-mounted NVG as it is possible to view the outside

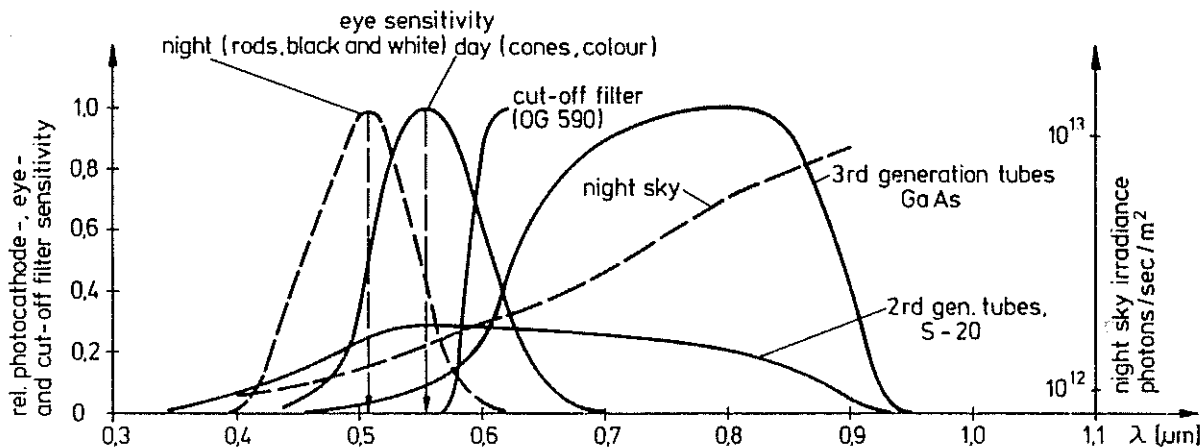


Fig. 23: Sensitivity of 2nd and 3rd gen. tubes, the eyes, a cut-off filter and the night sky irradiance functions of the wavelength

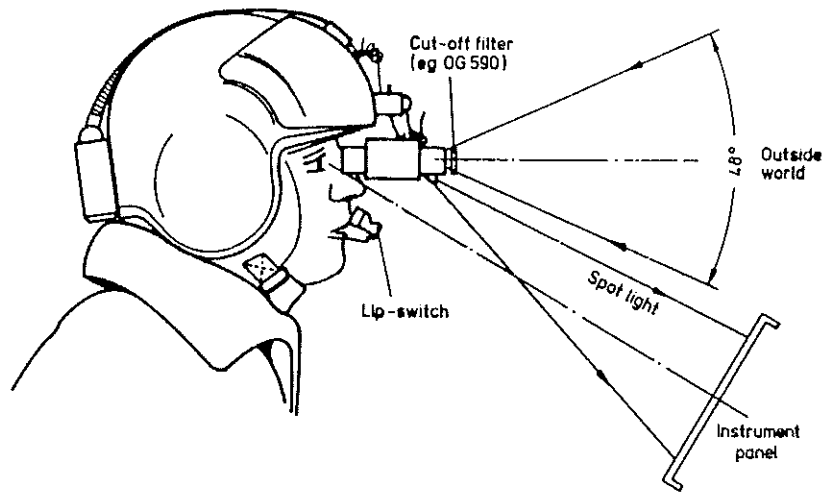


Fig. 24: Schematic view through and around helmet-mounted 3rd gen. NVG.
This helmet-mounted NVG was developed together with the German Army pilots

world through the goggles or to monitor instruments by looking "around" them. 3rd generation tubes have the advantage of amplifying overcast starlight in the longer wavelength (red and near IR) more efficiently than the 2nd generation tubes. The blooming effects are however also increased.

The PVS tests confirmed that NVG are a very attractive and cost-effective approach to assisting the piloting task during many night conditions. Under some conditions, e.g. poor visibility (fog) or heavy rain, they are still not as effective as advanced infrared cameras, however the pilot can quickly realize a degradation in their performance and is able to react accordingly. No problems exist in the NVG with temperature crossover points, which may give rise to obstacles disappearing for a time in thermal images.

4. Description and results of PISA

The companies involved in the project were EGO for the FLIR, MBB Dynamics Division for the platform, Koyo for the 12" black and white HDD and VDO for the SG. The new Cruise symbology was developed by MBB together with VDO. The system integration and flight tests were again conducted by MBB Helicopters Division.

Fig. 25 shows the nose-mounted platform, PISA, with the wide-angle FLIR. The cockpit with a HDD was screened off for simulated night flights. A beeper switch on the collective stick was used for platform steering in AZ and EL.

The platform parameters are:

- o type PISA
- o dimensions: 345 mm \varnothing x 470 mm without platform mounting
- o displacement angles: AZ \pm 90°; EL + 20° / - 45°
- o slew rate: max. approx. 1 rad/sec, variable
- o angular acceleration: max. 20 rad/sec²
- o mass: platform 19.3 kg and electronics 7.8 kg

The parameters of the FLIR are:

- o type PISA
- o spectral region: 8- 13 μ m
- o FOV: 30° x 60°, EP \sim 12 mm
- o IFOV: 1.7 mrad
- o magnification: x1
- o TED (Sprite)-detectors (62.5 x 700 μ m) cooled by nitrogen supplied from a 6 litre bottle
- o quasi serial/parallel scanning (Bouwers lens)
- o polygon, n = 8, 244 Hz
- o CCIR standard
- o mass: prototype FLIR 12.4 kg and electronics 10.4 kg
- o continuously variable contrast and brightness controls

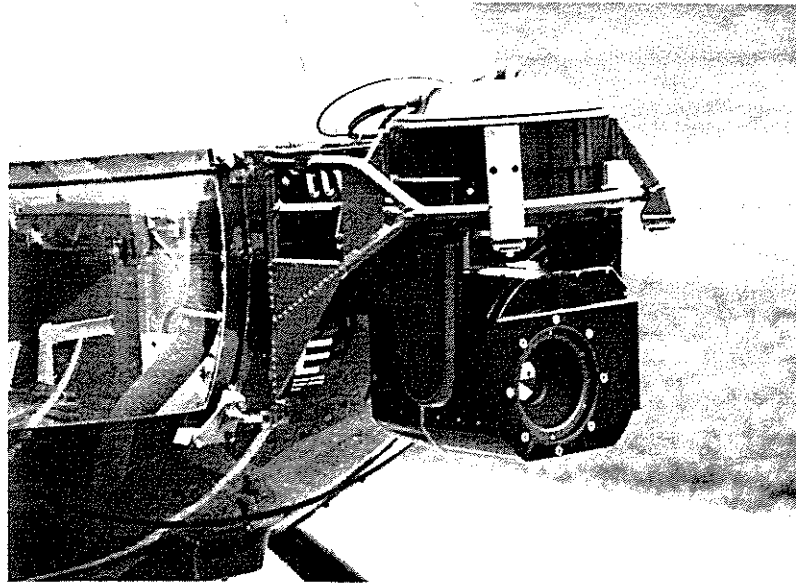


Fig. 25: Bo 105-S1 with the nose-mounted platform PISA (MBB) incl. FLIR (EGO) with 30° x 60° FOV

The computer generated flight symbology is shown in Fig. 26. It is a new Cruise symbology, superimposed on the FLIR image on the HDD. As the ratio of the FLIR image is 1:2 there is space left in the CCIR standard TV picture (3:4) for a band of symbology in the lower portion of the picture. No problems exist with the symbology brightness in the band, but the pilots did mention that the analogue radar altitude and rate of climb symbology should be displayed vertically and not horizontally. They were generally satisfied with the other symbols.

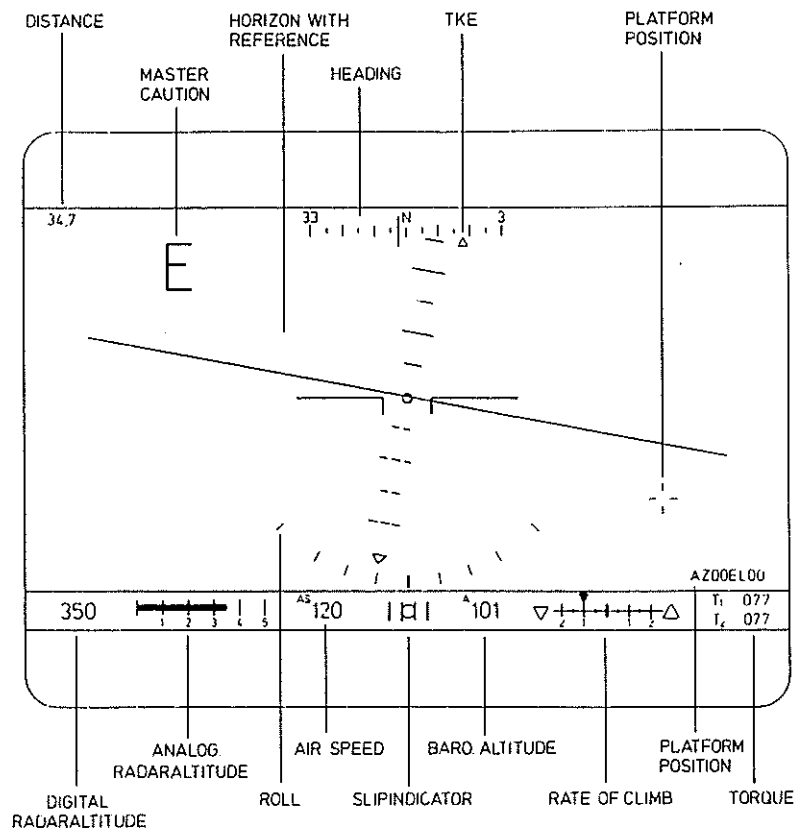


Fig. 26: Cruise symbology (PISA) with an information band in the lower portion of the picture

A few examples of the PISA flight trial results are shown in Figs. 27 and 28. They were recorded in the daytime (a.m.) in the month of April under good weather conditions. The FLIR images appear 3-dimensional with clearly defined shadows of the trees or houses. The superimposed Cruise symbology can be read quite well. It is possible to observe objects at a fair distance, even though the FLIR has a wide FOV of 30° x 60°. The tests showed that the platform displacement angles chosen were very good, especially in combination with the FOV of the FLIR. The manual steering of the platform by means of a beeper switch on the collective stick needs a great deal of experience in order to coordinate the platform AZ and EL movements. Simple flight manoeuvres are possible with PISA but terrain following and NOE flights are not possible without excessively increased pilot work load. In this case, an HMS coupled system or NVG are much easier to use. The variable slew rate and the reset switch on the collective stick were found quite satisfactory.

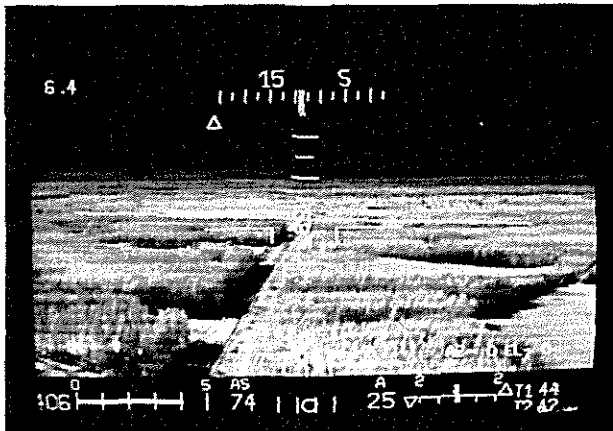


Fig. 27:

PISA FLIR image (30° x 60°) with superimposed Cruise symbology. Woods, a railway and a village in the background

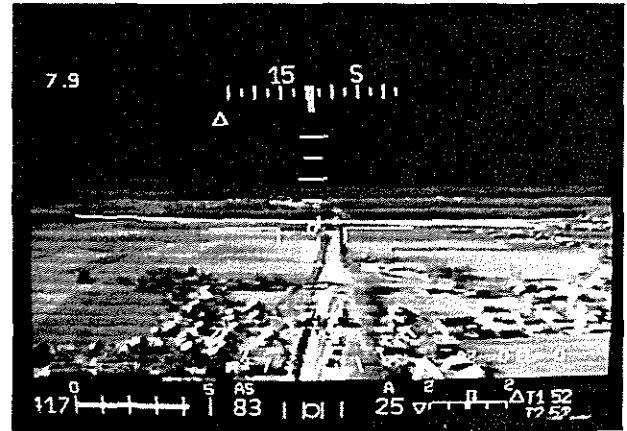


Fig. 28:

see Fig. 27, a village in front of the helicopter. 417 ft GND, 83 kts airspeed, T1, T2 = 52 % and heading 162°

5. Summary

With the experience gained from three different visionics programmes, including flight tests, it is now possible to equip future helicopters with adequate visionics systems for missions at night or in bad weather conditions.

For piloting tasks, the complexity of system depends on the mission requirements. Some possible major configurations for the piloting task are compared in Table 3. Considerable differences are of course also possible in the technology of the actual electro-optical sensor and thus within each configuration, there also exist a number of possible solutions. The weight and cost figures given for configurations 1 and 4 are only representative figures to give a feeling for the order of magnitudes involved.

In the PVS trials a rather complex system corresponding to configuration 1 was tested and found to fulfil most of the requirements for night flying. One critical aspect which is not solved with sufficient reliability is the detection of smaller obstacles like cables or wires. It should be noted that these hazards also cause problems under daylight conditions. However, MBB has also carried out successful flight tests with an experimental radar obstacle warning system developed by AEG-Telefunken. The development is continuing at present and further flight tests are planned.

① FLIR/LLTV nose-mounted position steerable platform (not stabilized) HMS/D	approx. 80 kg (DM) cost ≈ 500.000,-
② same as ① except now only HDD instead of HMS/D, platform control by beeper switch or automatic helicopter roll coupling	
③ same as ② except fixed installation for platform	
④ helmet-mounted NVG	approx. 1.5 kg (DM) cost ≈ 25.000,- / 2nd/3rd gen. 60.000,-

Table 3: Major configurations for piloting

Further aspects are the redundancy and limitations of the two basic principles, infrared temperature detection or light intensification. Thus the FLIR is not usable during conditions with hardly any temperature differences, which can be caused e.g. by steady or heavy rainfall. The NVG require a minimum illumination (0.5 - 3 mLux), depending on the type of goggles, for proper operation. During tests, conditions have been encountered where the FLIR reached its limits. On one occasion, in very heavy rainfall, both technologies did not allow continuance of the mission. Nevertheless, it is felt that a combination of the two dissimilar technologies, i.e. a FLIR and NVG, is an excellent cost-effective combination, when high mission reliability is required.

In the case of a night observation system also being required, another approach is of course to add a third large field of view to the observation system, using this channel as back-up for piloting. This is also true, when the observation system is in the mast-mounted configuration as shown in Fig. 29. Owing to parallax, the LOS has then to be moved automatically in the downwards direction, in order to view an obstacle at a short distance from the blade tip. The image becomes larger, but rotor blade influences is seen only as a "chopper" effect occurring in addition (ref. 6).

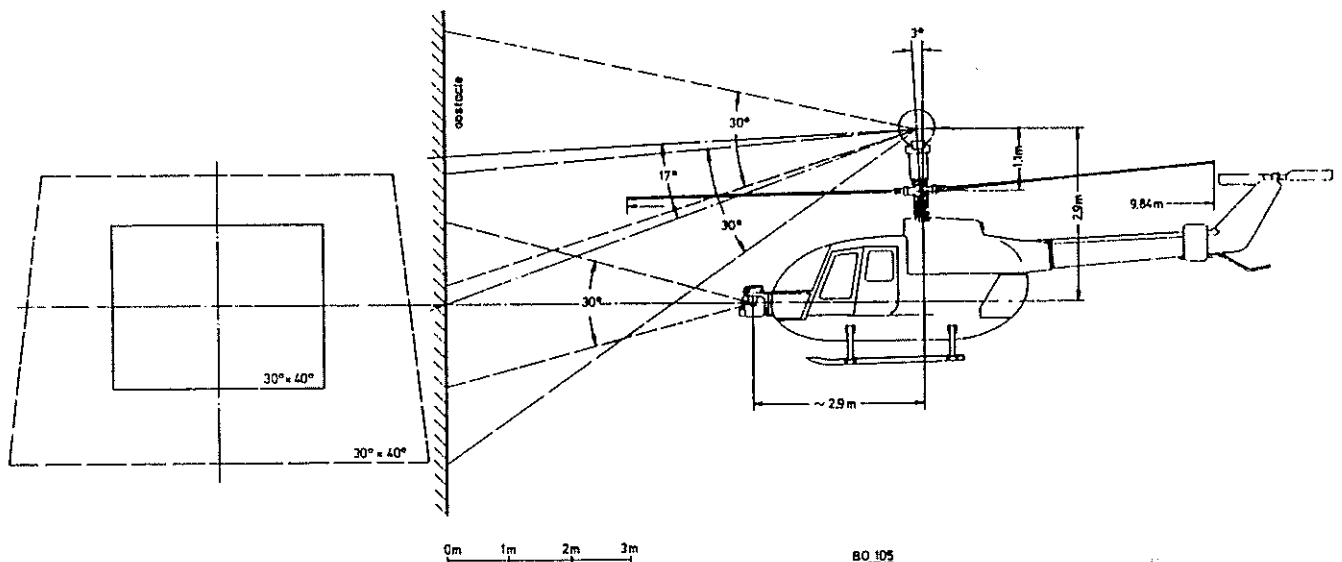


Fig. 29: Comparison of the image size for a 30° x 60° FOV FLIR in the nose and mast-mounted configuration, close to an obstacle

In the tests the FLIR gave a generally better image when directly compared with the LLLTV camera. On the whole, it is not possible to judge the exact distance, particularly on landing, with either FLIR, LLLTV or NVG. The results with the electro-magnetic HMS were very satisfactory. The monocular HMD was also, in general, good.

The experiments with the two different NVG have demonstrated that NVG are a strong contender for a large number of applications and offer a cost-effective solution for piloting tasks.

For future helicopters used for observation, a FLIR equipped with a telescope on a mast-mounted platform like OPHELIA, is technically a good solution, providing a periscopic sight with a nearly unlimited 360° viewing.

6. Abbreviations

AFCS	Automatic Flight Control System
ANVIS	Aviators Night Vision Imaging System
AZ	Azimuth
BMFT	Bundesministerium für Forschung und Technologie
CALIPSO	Caméra Légère Infra-rouge Pour Systeme OPHELIA
CCIR	European video standard with 625 lines, 25 Hz frame rate
CEP	Circular Error Probability
CRT	Cathode Ray Tube
EL	Elevation
EP	Entrance Pupil
FLAB	Flying Laboratory
FLIR	Forward Looking Infrared
FOV	Field of View
HDD	Head-down Display
HMD	Helmet-Mounted Display
HMS	Helmet-Mounted Sight
HMS/D	Helmet-Mounted Sight/Display
IAS	Indicated Air Speed
IFOV	Instantaneous Field of View
IFR	Instrument Flight Rules
IR	Infrared
LLLTV	Low Light Level TV camera
LOS	Line Of Sight
NOE	Nap of Earth
NVG	Night Vision Goggles
OPHELIA	Optique sur Plate-forme HELICOPTÈRE Allemand
PISA	Piloten Infrarot Sicht-Anlage (pilots infrared system)
PVS	Pilot Visionics System
SG	Symbol Generator
SPRITE	Signal Processing in The Element (TED)
TED	Tom Elliott Device (SPRITE)
VFR	Visual Flight Rules

7. Reference

- 1) G.F.H. Lloyd: Helicopter cockpit design for night goggle compatibility. Presented at the Sixth European Rotorcraft Forum, Paper No. 64, Bristol, England, 16-19 Sept. 1980
- 2) R.-D. v. Reth, M. Kloster: Mast Mounted Visual Aids. Presented at the Seventh European Rotorcraft Forum, Paper No. 53, Garmisch-Partenkirchen, FRG, 8-11 Sept. 1981

- 3) R. Beyer, E. Danneberg, E. Kohnen, H. Stein: Experimental Investigation of visual aids vor helicopters low level flight at night and poor visibility. Presented at the Seventh European Rotorcraft Forum, Paper No. 54, Garmisch-Partenkirchen, FRG, 8-11 Sept. 1981
- 4) H. Hesse: Erweiterung der Nachteinsatzfähigkeit der Heeresflieger durch Bildverstärker-Brillen. Presented at the 14. Internationales Hubschrauber Forum, Bückeberg, FRG, 20-21 May 1982
- 5) K. Schymanietz, H.-D.V. Böhm: Nachteinsatz militärischer Hubschrauber, Analyse und Ausblick. Presented at the 14. Internationales Hubschrauber Forum, Bückeberg, FRG, 20-21 May 1982
- 6) H.-D.V. Böhm: Bo 105 rotor blade influence on the CALIPSO FLIR in the mast-mounted observation platform OPHELIA. Presented at the Eigth European Rotorcraft Forum, Paper No. 11.7, Aix-en Provence, France, Aug. 31 through Sept. 3, 1982
- 7) W. Metzdorf, H. Hauck: Low Level flight and navigation at night in central Europe. Presented at the Eigth European Rotorcraft Forum, Paper No. 12.6, Aix-en Provence, France, Aug. 31 through Sept. 3 1982
- 8) J. Barrett: Night and poor weather helicopter offshore operations. Presented at the Offshore Helicopter Operating Safety Seminar, Brighton, England, 19-20 Oct. 1982
- 9) R.-D. v. Reth: Untersuchungen und Entwürfe für ein neues Hubschrauber Cockpit Presented at the 3. BMFT Statusseminar, Hamburg, FRG, 2-4 May 1983
- 10) R.-D. v. Reth: Development of avionic systems for future helicopters. Presented at the 39th Annual Forum of the American Helicopter Society, St. Louis, Missouri, 9-11 May 1983
- 11) MBB brochure: The Flying Laboratory Bo 105, Future Avionics & Visionics Systems, May 1983